

May 2016

Increasing the acceptance rate of $H \rightarrow 4e^-$ Run 1 events by relaxing the applied cuts

Beni J. Pazar

Macalester College, bpazar@macalester.edu

Abstract

The Decay mode of Higgs into four leptons allows for accurate parameter reconstruction and is thus a useful channel to research. The study attempted to increase the number of four electron events that pass selection cuts, without greatly increasing the amount of background noise, by varying the transverse momentum, invariant mass of the subleading electrons, and electron identification. With the application of a boosted decision tree targeting the ZZ^* noise, the study found that the optimal configuration was a loose electron identification with the invariant mass greater than 10 GeV and the transverse momentum greater than 7 GeV.

Follow this and additional works at: <http://digitalcommons.macalester.edu/mjpa>

 Part of the [Physics Commons](#)

Recommended Citation

Pazar, Beni J. (2016) "Increasing the acceptance rate of $H \rightarrow 4e^-$ Run 1 events by relaxing the applied cuts," *Macalester Journal of Physics and Astronomy*: Vol. 4: Iss. 1, Article 7.

Available at: <http://digitalcommons.macalester.edu/mjpa/vol4/iss1/7>

This Capstone is brought to you for free and open access by the Physics and Astronomy Department at DigitalCommons@Macalester College. It has been accepted for inclusion in Macalester Journal of Physics and Astronomy by an authorized administrator of DigitalCommons@Macalester College. For more information, please contact scholarpub@macalester.edu.

Increasing the acceptance rate of $H \rightarrow 4e^-$ Run 1 events by relaxing the applied cuts

Cover Page Footnote

Thank you to R.D. Schaffer for all of his continued help.

The Standard Model Higgs Boson

The Higgs Boson is the final missing piece of the Standard Model (SM). With this final piece added by Robert Brout, Françoise Englert, and Peter Higgs (BEH), the Standard Model was able to describe the three families of fundamental particles and their interactions¹. Each force's effective range is inversely proportional to the mass of its respective mediating boson. The electromagnetic force is mediated by the photon, which has no mass, and thus the electromagnetic force has an infinite effective range. The Weak force, responsible for radioactive decay, has a very small effective range and consequently has a very heavy mediating boson. However, before BEH, the Standard Model could not explain any particle's mass. Rather, it predicted that all particles were massless. This was overcome through the introduction of the Higgs Field. The stronger a particle coupled with the Higgs field the more massive it was.

The BEH mechanism worked using the principle of spontaneous symmetry breaking of the electroweak field. The scalar field had a zero vacuum expectation value up until 10^{-11} seconds after the Big Bang, like all other fields. At that moment, the field acquired a nontrivial value¹. This symmetry breaking allowed the Higgs field to couple with other particles, and by extension give them mass. The BEH addition to the Standard Model allowed for the accurate prediction of the W and Z boson mass, while leaving the photon massless². The final prediction of the BEH theory was the existence of a particle³, with non-predicted mass, called the Scalar Boson or Higgs Boson.

¹ The Standard Model does not include Gravitational effects and as such is an incomplete theory of the universe.

² The W and Z boson were experimentally confirmed in 1983 at CERN by the experiments UA1 and UA2.

On July 4th 2012, CERN announced the experimental verification of a Higgs-like particle. After the completion of Run 1 of the Large Hadron Collider (LHC), approximately 50 years after the prediction of the BEH theory, the Higgs boson was found. It is possible that the particle discovered does not exactly match what was predicted by BEH theory. In this paper the particle discovered by ATLAS and CMS will be referred to as the Higgs boson.

The Higgs Boson And The Detector

Particles which are accelerated through the LHC are collided at the center of the ATLAS⁴ detector. Run 1 collided particles at a center of mass energy of 7 and 8 TeV. All collisions occurring after the upgrade to center of mass collisions at 14 TeV will be classified as Run 2. There are four modesⁱⁱ of Higgs boson production at the LHC. Gluon-gluon fusion (ggF) $gg \rightarrow H$ has the largest production likelihood. Due to their lack of mass, gluons are not able to directly couple with the Higgs boson, rather; they produce loops with heavy particles, which in this case are W bosons and top quarks. Next, there is the vector boson fusion (VBF) $qq \rightarrow Hqq$. In this case, the Higgs boson is produced in conjunction with two energetic jets. Finally, there are the cases where the Higgs boson is produced with either a vector boson, called Higgs-Strahlung (VH), or produced along with top quarks ($t\text{-}\bar{t}H$)⁵.

The Higgs boson can decay in many ways, preferring modes where the Higgs boson couples to the most massive particles possible. Though certain states may have a larger likelihood, decay modes with the highest signal to noise (S/N) ratios are preferred. Such examples are the decays modes of the Higgs boson into $b\text{-}\bar{b}$ quarks and $\tau\text{-}\bar{\tau}$ leptons.

³ Like all other fields in Quantum Field Theories, excitation of the field produces particles.

⁴ **A Toroidal LHC ApparatuS**

⁵ Figure 2

Both are very likely modes for the Higgs boson to decay. Yet due to the difficulty of distinguishing jets and b quarks, due to resolution of the energy in the hadronic calorimeter and also the difficulty of QCD process modeling, other decay modes are preferred.

For a Higgs boson of mass 125 GeV, the decay into four leptons ($H \rightarrow ZZ^* \rightarrow 4l$) has a very small decay likelihood. However, this decay mode is studied, because of the small and controllable background noise. I have focused my research on the decay mode of the Higgs boson into four electrons ($H \rightarrow ZZ^* \rightarrow 4e$). This decay mode is interesting because it allows us to measure the properties of the detected Higgs boson. Due to the low rate of background noise in the signal zone, there is high resolution for the reconstructed mass and good analysis opportunities of spin. I studied the Higgs decay into four electrons because the efficacy of their reconstruction and selection is much smaller than that of muons.

The ATLAS Detector

The ATLAS detectorⁱⁱⁱ has near forward-back cylindrical symmetry. It has three main areas: the inner tracking detector (ID), the calorimeters, and the muon detector⁶. The regions detect increasing energy, facilitating the three-level trigger system. The ID is comprised of a silicon pixel detector placed near the particle interactions. Surrounding the ID is a silicon microstrip detector. Both of those sections are covered by a transition radiation straw-tube tracker (TRT). The calorimeter is split into two subsections. An electromagnetic calorimeter comprised of liquid argon (LAr) and a hadron calorimeter constituted from iron scintillating

⁶ Figure 3

tiles. The final level ring is the muon spectrometer. The spectrometer consists of one barrel with two endcap regions mainly consisting of cathode strip chambers.

Background Noise

All processes whose final states are the same as the signal⁷ but were not produced by a Higgs boson decay are classified as noise. The two major types of noise are the irreducible ZZ^* production and the reducible false detection of electrons. The ZZ^* is irreducible because it does not arise from a misidentification. There are many other ways for a ZZ^* pair to be produced other than Higgs boson decay. Any ZZ^* pair, no matter the origin, can decay into four leptons and thus mislead the reconstruction.

There are three main processes that produce the reducible misidentified final states⁸. In the first case $Z(ee)+bb\bar{b}$, the semi-leptonic decay of b quarks yields non-isolated electrons along with electrons produced from Z boson decay. In the second case $W(ev)Z(ee)+jets$, there are electrons produced from Z and W boson decay along with jets that are misidentified as electrons. This misidentification occurs because the jets are predominantly composed of charged particles and the combined use of the LAr detector for both charged leptons and charged hadrons.

The Goal

After selection cuts are applied Higgs decay into four leptons only 40% of 4μ events remain and less than 20% remains for $4e$. The reason for the drastic difference is the due to

⁷ In this study the final state is two electron-positron pairs.

⁸ $Z(ee)+bb\bar{b}$, $W(ev)Z(ee)+jets$, $Z(ee)+jets$

the harshness of the selection cuts biased against noise. Because the electrons have lower energy than muons the cuts are more restrictive. The question posed by this research was to see if we could increase the number of 4e- events, without losing statistical significance⁹, by relaxing the selection cuts.

Three selection parameters were varied; the minimum transverse momentum (P_t) of electrons^{iv}, the minimum reconstructed mass of the sub-leading electron pair, and finally the looseness of the electron likelihood. The selection cut on the P_t of the lowest energy electron (e_4) was varied from 7 to 6 and 5 GeV. Though this allowed more events to pass through, the noise increases greatly at lower energies. The second selection cut was applied to the invariant mass of the subleading electron pair. The cut was varied from 12 to 10 and 8 GeV.

The final selection cut was the type of electron identification that was applied. The more stringent the parameters the higher the rejection of both true and misidentified electrons. In Run 1 the electron identification used was strict and referred to as “normal”. This electron identification was able to reduce the noise events that passed from Z+jets to fewer than those from ZZ*. The question analyzed was if it would be able to relax the selection cuts, and thus gain more events, without a reduction in the statistical factor \hat{Z} .

Finally, there was another discriminator that was applied to all events: a Boosted Decision Tree (BDT). The BDT looked at many parameters of each event, and based on a complex sorting mechanism, is able to ascribe value to the event. Based on the value of the

⁹ The measure of significance used: $\hat{Z}=\sqrt{2[(s+b)\ln(1+s/b)-s]}$ Cowan&Gross, 2008

event there is a certain probability that the event either contains real or false electrons.

The main parameters that the BDT takes into account are the momentum, pseudorapidity, and mass of the particles. Only events with a BDT value greater than zero were kept. This process mirrors what was done by the ATLAS in their analysis of the Run 1 data¹⁰.

Selection Variation Analysis

The constructed events were required to pass through the standard selection cuts prior to any of the cuts being tested were applied. The number of generated events were then normalized to the data¹¹ from Run 1 at an integrated luminosity of 20.3 fb^{-1} . The selection cuts were first applied to purely the ZZ^* noise events, then to the Z+jets events, and finally to a noise constituted from their combination. In a preliminary look, it was found that the number of ZZ^* events grew when all three studied selection cuts were loosened. For the P_t the largest significance was found at 5 GeV, though there was also an improvement at 6 GeV.

To study the effects of the cuts purely on the Z+jets events, an approximation was required. It was necessary to set up a control region where the loose electron identification could be applied. To produce the events that passed the selection cuts in the signal zone an extrapolation was made from the control region to the signal region. The extrapolation process had a minimum of 60% systematic uncertainty. This process was used, despite such a high systematic uncertainty, because it was the best way to study the loose electron identification on Z+jets events.

¹⁰ The BDT used only discriminated against ZZ^* noise.

¹¹ $4e$: signal=2.379; ZZ^* =1.03; Z+jets=0.35; \hat{Z} =1.1776

After 2012 a new electron identification was implemented that biased the likelihood of real electron production against jets produced from Z bosons. The use of the loose-likelihood identification was able to reject twice as many jet events.

Statistical Results

There were three stages of analysis: the irreducible noise (ZZ^*), the reducible noise (Z+jets), and finally their combination. For the first round of tests we found that the best value for the P_t was 5 GeV, when combined with the standard electron identification. With the loose electron identification the optimal cut on the P_t became 6 GeV. For the invariant mass (M_{34}) the optimal cut was at 10 GeV for all values of P_t and electron identification. When looking at purely the ZZ^* events a looser electron identification than what was used for Run 1 analysis always augmented the number of signal events more than the increase in ZZ^* noise.

For the second step we looked at the effects of lowering the selection cuts on the reducible noise produced from Z+jets. The optimal cut on the P_t was the standard 7 GeV for all configurations. As with the irreducible background noise, the optimal cut for the invariant mass (M_{34}) was at 10 GeV. There was no way to construct a signal region from the control region using the standard electron identification, and thus all data for the Z+jets events were only tested with the loose electron identification. The loose electron identification was better for the irreducible background noise and so it is a fairly safe assumption that it will also be better for the reducible noise.

Conclusion

The ideal selection parameter configuration is as follows: $P_t=7$ GeV, $M_{34}=10$ GeV, and the loose electron identification. Though a lower P_t cut was optimal for the ZZ^* noise, the gains were outweighed by the losses from Z+jets. We can see in Figure 6 that for the Z+jets there is a very large number of events below the 7 GeV threshold.

For future research there are multiple areas of improvement, but also many new opportunities due to the upgrade of the LHC. To begin, there is still much that should be done concerning the reducible noise from the Z+jets. The BDT used was calibrated for the ZZ^* noise and is thus not very effective against the reducible noise. Though a Z+jets BDT could be constructed, the time and effort required would not be worth the gains in significance. As previously stated, only the loose electron identification was used on the Z+jets. Though this identification is most likely better and produced significant gains, we cannot draw any strong conclusions.

This study only looked at the two most prevalent types of noise in the H4e- mode. Though they are far less significant, it would be useful to look at how effective the new selection cuts would be against the other types of noise. The types of noise disregarded were $t\bar{t}$ and WZ boson noise. Though less prevalent, $t\bar{t}$ noise behaves similar to the Z+jets and thus could reduce the significance a little more.

The motivation for lowering the selection cuts on the H4e mode was the prior success with the 4μ . The decay mode $2\mu 2e$ has electrons as the subleading pair, similar to this study, and so it is reasonable to think that the $2\mu 2e$ mode would benefit from similar

changes. A direct study would need to be conducted to be certain, but this would be simple and very beneficial.

The LHC was upgraded to a center of mass energy of 14 TeV for Run 2 in 2015. With the higher energy collisions, lowering the selection cuts on the leading electrons (not just subleading) became viable. The higher luminosity will, of its own accord, increase the significance of Higgs detection. It is still beneficial to have the largest significance possible so as to facilitate the reconstruction of the Higgs properties more precisely. Preliminary investigations of lowering the electron identification to an even looser setting showed promise.

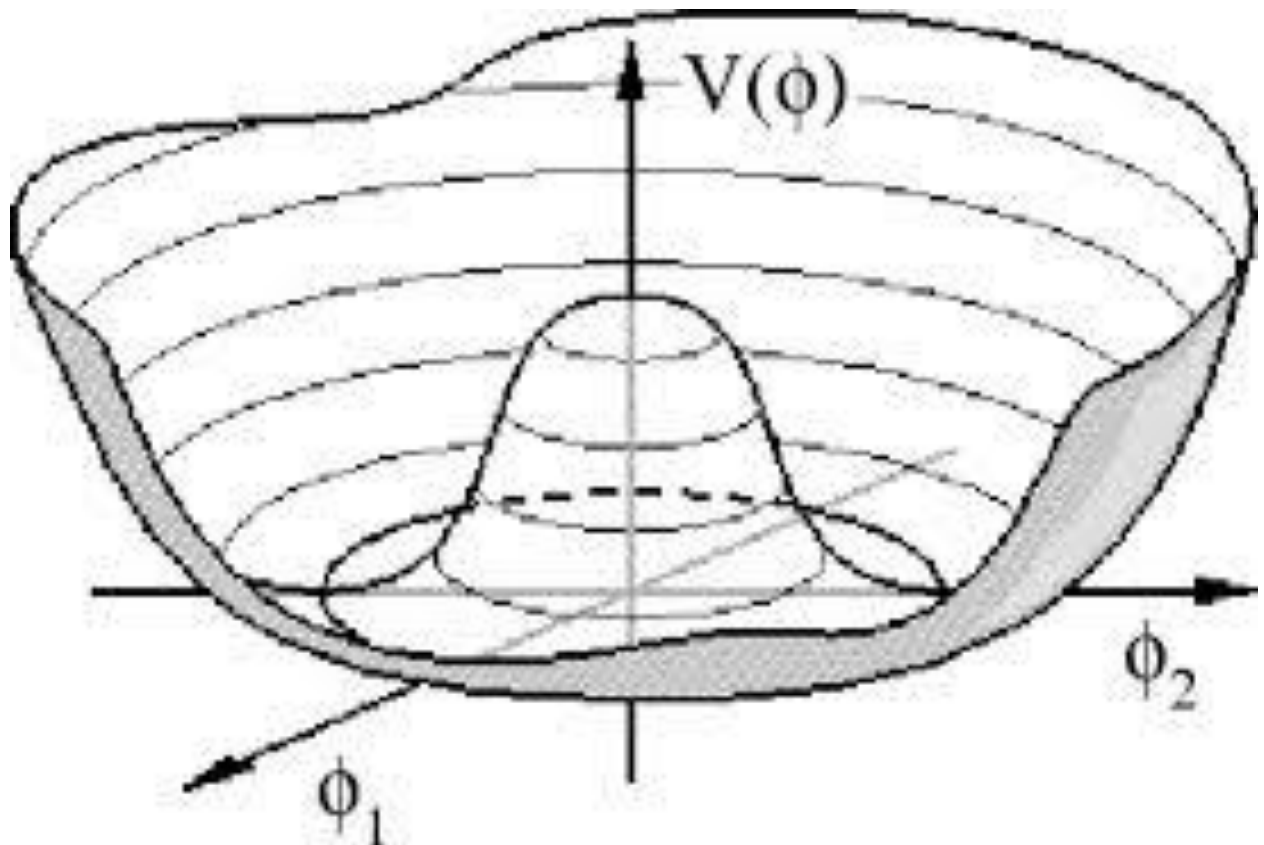


Figure 1. The Higgs potential. The divit in the middle maintains the azimuthal symmetry while breaking the transverse symmetry. Picture courtesy: E.P.S. Shellard, DAMTP, Cambridge.) From <http://www.geocities.com/CapeCanaveral/2123/breaking.htm>.

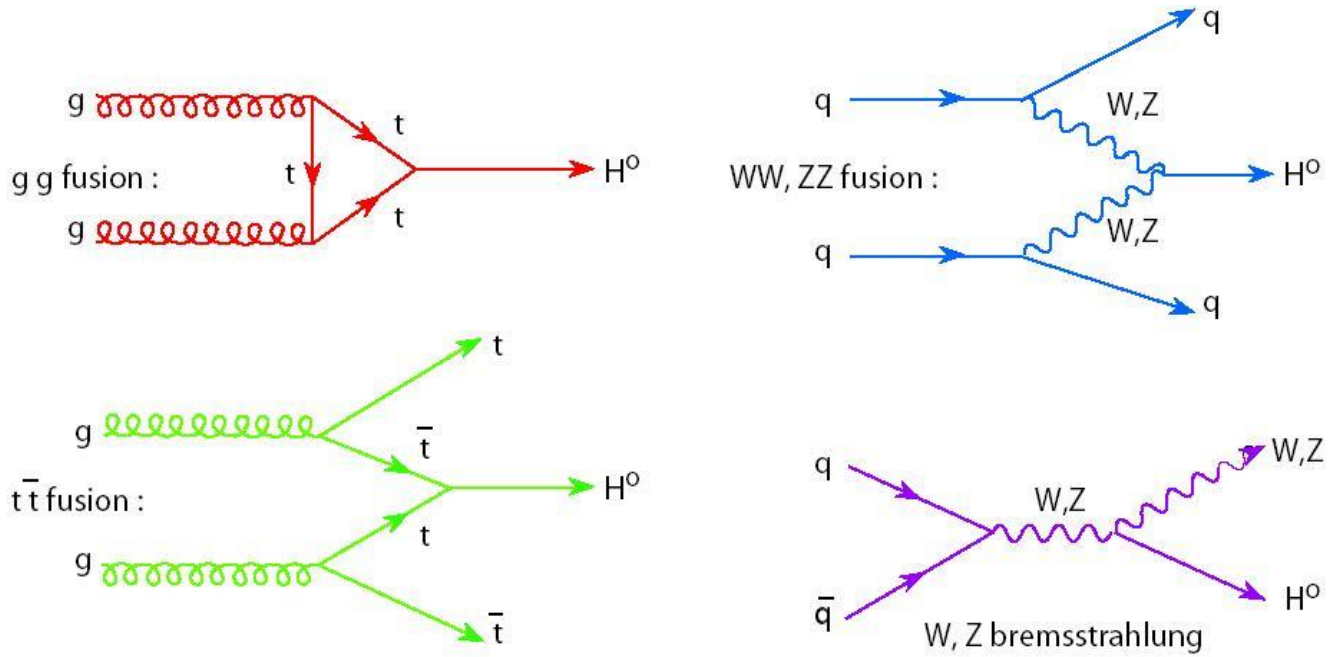


Figure 2. The main production modes for the Higgs Boson. This Study mostly looked at ggF which is the top-right.

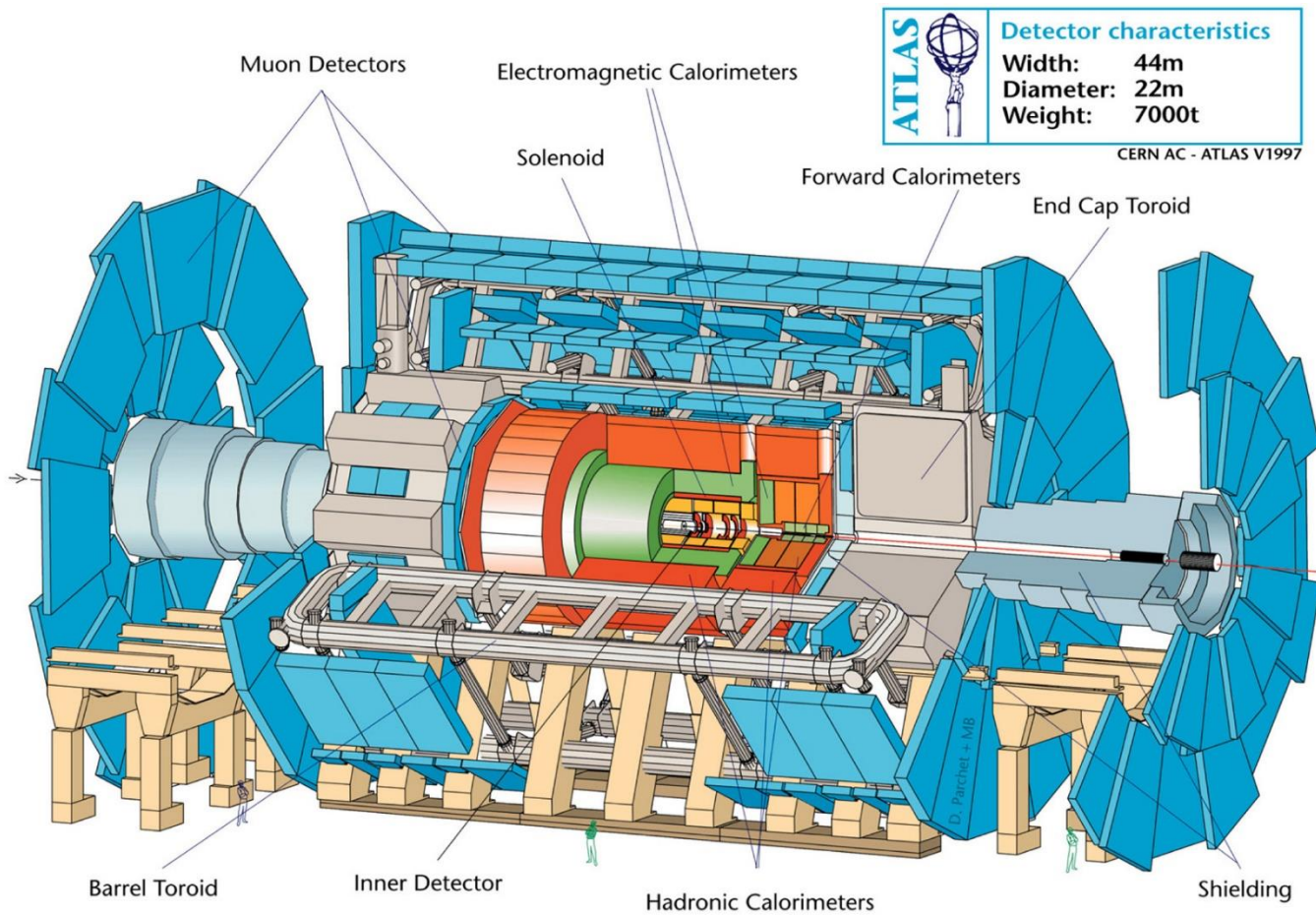


Figure 3. The ATLAS detector with all sections labeled and a person for scale. Picture courtesy: Alex Grillo, ATLAS) From <http://scipp.ucsc.edu/personnel/atlas.html>.

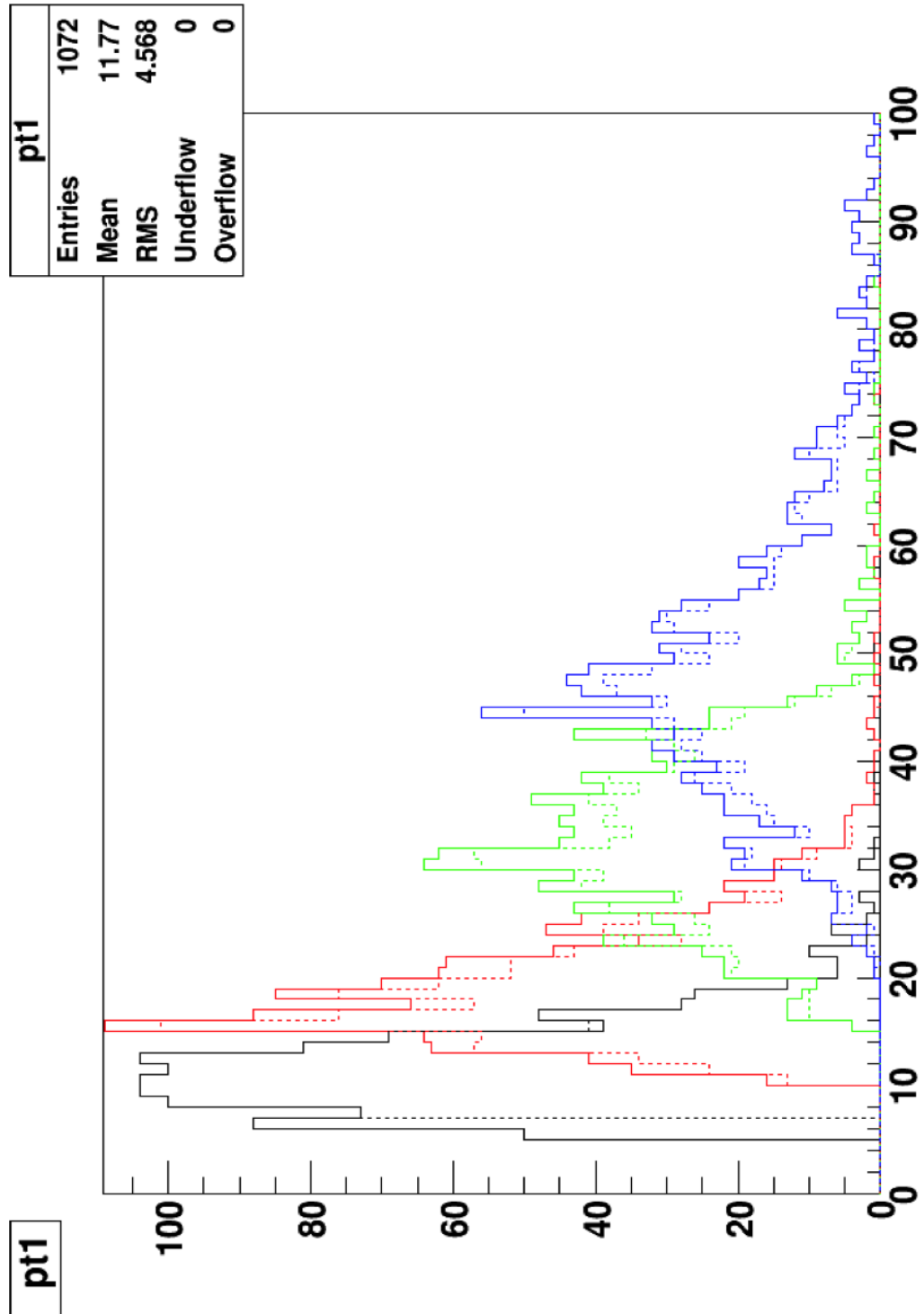


Figure 4. The Transverse Momentum distribution of the four electrons. The dotted line is

for the 7 GeV cut while the solid line is at 5 GeV. We can see that there are a few events to be gained by lowering the cut.

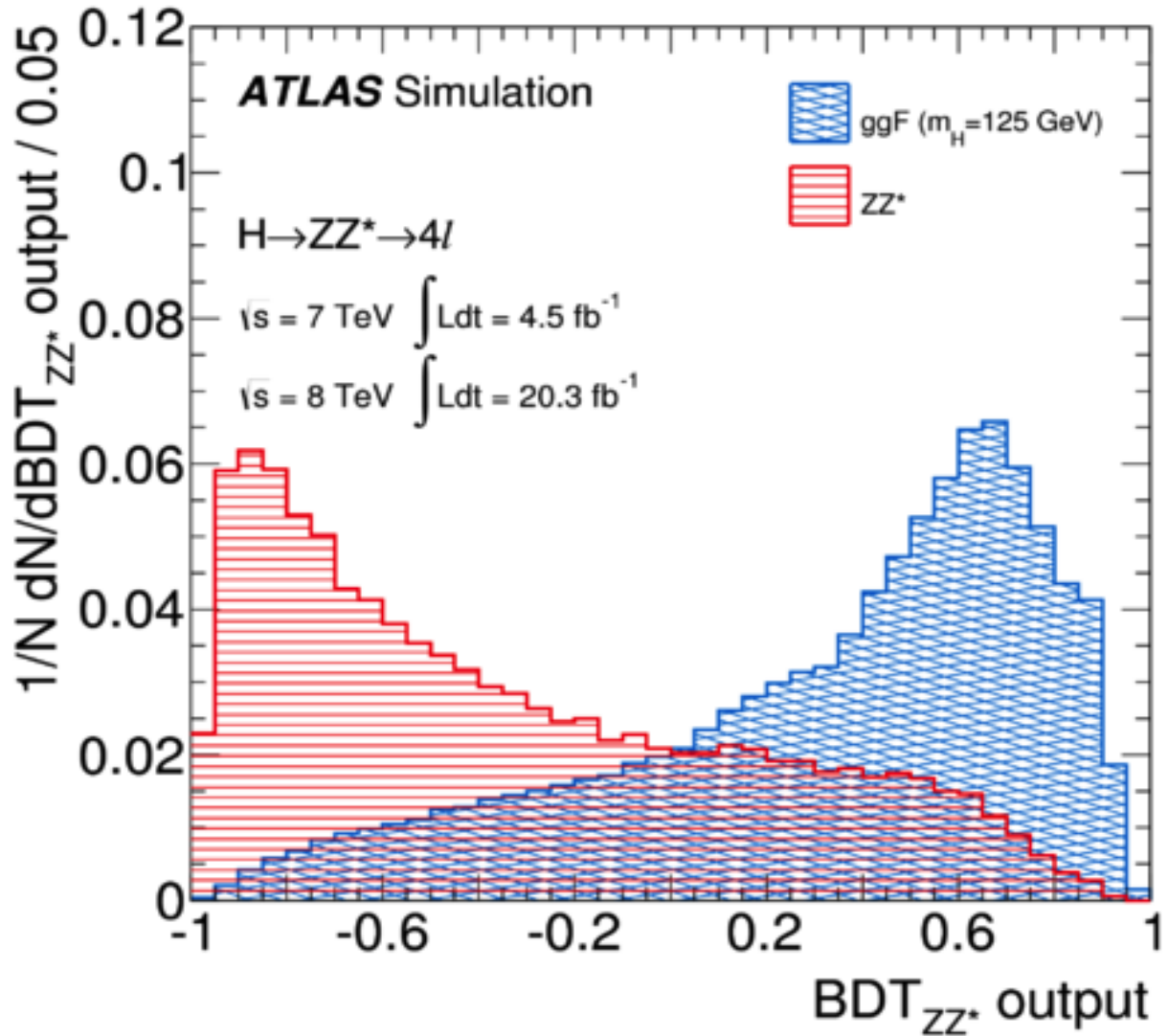


Figure 5. DBT discriminating against ZZ* noise. The cut required all events to have a BDT value greater than 0. The BDT was thus able to reduce the noise by a factor of 2/3 while only loosing 1/3 of the signal.

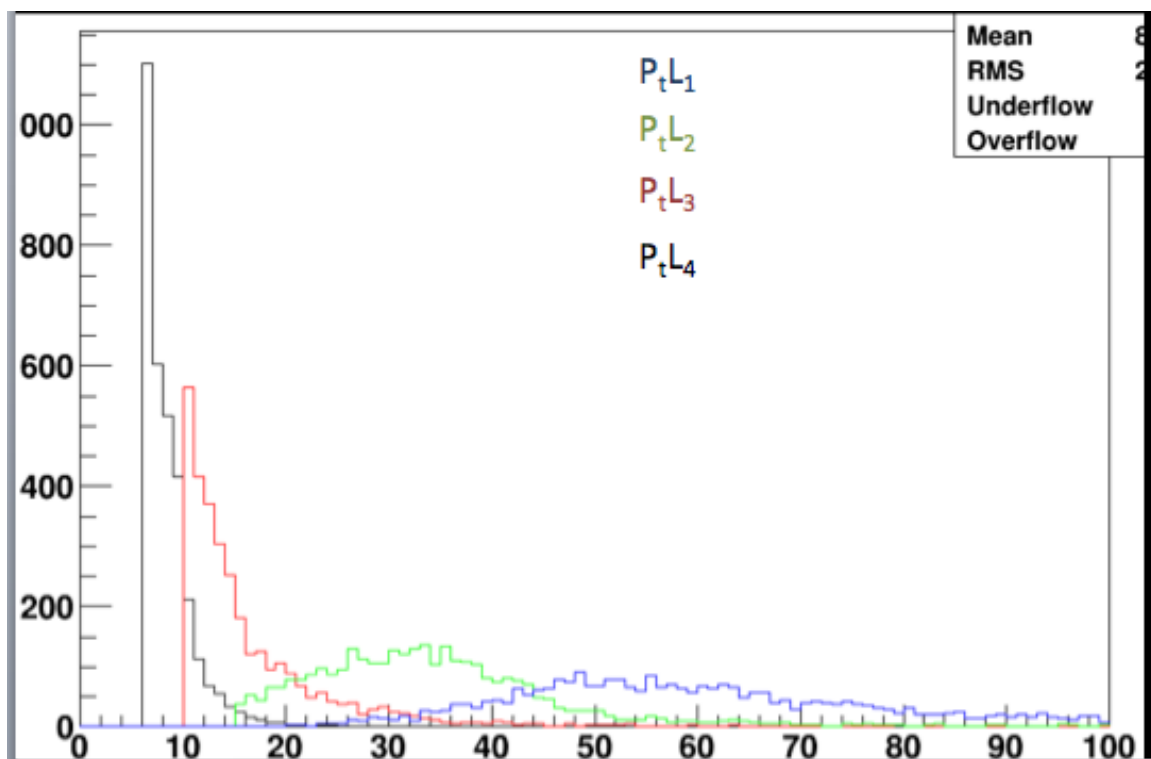


Figure 6. The probability density of the four electrons produced from Z+jets events as a function of mass in GeV. We can see that there is a sharp spike in the noise bellow 7 GeV, the placement of the original selection cut.

Table 1: 20.3 fb^{-1} & Loose & $M_{34} > 12$ & $BDT = \emptyset$

	5 GeV	6 GeV	7 GeV
<i>Signal</i>	3.073	2.943	2.712
<i>ZZ*</i>	1.633	1.442	1.229
<i>Z + jets</i>	0.645	0.577	0.350
<i>BDF_{total}</i>	2.278	2.019	1.579
<i>Z</i>	1.730	1.743	1.776
<i>%increaseSignal</i>	+29.172%	+23.707%	+13.997%
<i>%increaseZZ*</i>	+58.390%	+39.864%	+19.205%
<i>%increaseZ + jets</i>	+84.286%	+64.857%	+00.000%
<i>%increaseBDF_{total}</i>	+44.269%	+27.866%	00.000%
<i>%increaseZ</i>	-2.590%	-1.858%	00.000%

Table 1. The control table. All cuts are standard and no BDT is applied. BDF denotes the combined ZZ* and Z+jets noise.

Table 2: 20.3 fb^{-1} & Loose & $M_{34} > 12$ & BDT >0.0

	5 GeV	6 GeV	7 GeV
<i>Signal</i>	2.370	2.307	2.165
<i>ZZ*</i>	0.517	0.481	0.441
<i>Z + jets</i>	0.369	0.357	0.232
<i>BDF_{total}</i>	0.886	0.838	0.673
<i>Z</i>	1.933	1.925	1.959
<i>%increaseSignal</i>	-0.378%	-3.026%	-8.995%
<i>%increaseZZ*</i>	-49.855%	-53.346%	-57.226%
<i>%increaseZ + jets</i>	+5.429%	+2.000%	-33.714%
<i>%increaseBDF_{total}</i>	-43.889%	-46.928%	57.378%
<i>%increaseZ</i>	+8.840%	+8.390%	+10.304%

Table 2. Standard cuts with the BDT applied.

Table 4: 20.3 fb^{-1} & Loose & $M_{34} > 10$ & $BDT > 0$

P_t	5 GeV	6 GeV	7 GeV
<i>Signal</i>	2.396	2.333	2.191
<i>ZZ*</i>	0.531	0.494	0.455
<i>Z + jets</i>	0.528	0.365	0.236
<i>BDF_{total}</i>	1.059	0.859	0.691
<i>Z</i>	1.838	1.927	1.962
<i>%increaseSignal</i>	-11.652%	-13.975%	-19.211%
<i>%increaseZZ*</i>	-48.497%	-52.085%	-55.868%
<i>%increaseZ + jets</i>	+50.857%	+4.286%	-32.571%
<i>%increaseBDF_{total}</i>	-32.932%	-45.598%	-56.238%
<i>%increaseZ</i>	+3.491%	+8.507%	+10.473%

Table 3. The M_{34} is set to be greater than 10 GeV. This is the optimal configuration.

Table 2: 20.3 fb^{-1} & Loose & $M_{34} > 12$ & BDT >0.0

	5 GeV	6 GeV	7 GeV
<i>Signal</i>	2.370	2.307	2.165
<i>ZZ*</i>	0.517	0.481	0.441
<i>Z + jets</i>	0.369	0.357	0.232
<i>BDF_{total}</i>	0.886	0.838	0.673
<i>Z</i>	1.933	1.925	1.959
<i>%increaseSignal</i>	-0.378%	-3.026%	-8.995%
<i>%increaseZZ*</i>	-49.855%	-53.346%	-57.226%
<i>%increaseZ + jets</i>	+5.429%	+2.000%	-33.714%
<i>%increaseBDF_{total}</i>	-43.889%	-46.928%	57.378%
<i>%increaseZ</i>	+8.840%	+8.390%	+10.304%

Table 4. The M_{34} is set to be greater than 8 GeV.

Bibliography

Measurements of Higgs boson production and couplings in the four-lepton channel in pp collisions at center-of-mass energies of 7 and 8 TeV with the ATLAS detector, The ATLAS Collaboration, 22/08/2014

Measurement of the Higgs boson mass from $H \rightarrow \Upsilon\Upsilon$ and $H \rightarrow ZZ^* \rightarrow 4l$ channels with the ATLAS detector using 25 fb^{-1} of pp collision data, The ATLAS Collaboration, 15/06/2014

Performance du calorimètre électromagnétique et recherche du boson de Higgs dans son canal de désintégration $H \rightarrow ZZ^* \rightarrow 4l$ avec l'expérience ATLAS, Élodie Tiouchichine, 10/10/2014

Discovery significance with statistical uncertainty in the background estimate, Cowan & Gross, 8/05/2008

ⁱ Figure 1. Higgs Potential

ⁱⁱ Figure 2. Production Graphic

ⁱⁱⁱ Figure 3. ATLAS detector

^{iv} Figure 4. Transvers Momentum electrons